

博士論文

**Sub-nanoscale Hydrophobic Modulation of
Salt Bridges in Aqueous Media**

(ナノスケールにおける疎水面による塩橋への影響)

陳 碩

General Introduction

The hydrophobic effect¹ – the tendency for non-polar molecules to aggregate in an aqueous solution – plays an important role from the cleaning of laundry to the creation of emulsions for cosmetics. Soon after its first introduction by Walter Kauzmann in 1959,² this water-mediated effect was referred by John Kendrew and Max Perutz (1962 Nobel Laureates) to explain the first atomic structure of a protein.³ Nowadays it is known that approximately 75% of the protein surface is covered by nonpolar amino acid residues, while 25% is covered by polar ones.⁴ Thus it is intriguing to consider how the diversity of molecular recognition can be developed from only a limited variety of polar residues in proteins. A theory by Schellman in the 1950s⁵ postulated that interactions between ionic species in aqueous media, when approaching a hydrophobic surface, would be enhanced. This theory suggests that varied local hydrophobic maps are probably harnessed by homologous proteins to combine with conserved polar interactions and develop distinct adaptive functions. However, the long-standing theory of Schellman lacks experimental proof to date. Difficulties lie in how to construct ion pairs located at a defined distance from a hydrophobic surface and how to quantify their strengths.

In my study, I elaborately designed a series of ionic head groups-appended fluorescent self-assembled monolayers fSAM_{C2}, fSAM_{C6}, fSAM_{C8}, and fSAM_{C12}, which are composed of C2, C6, C8, and C12 space-filling alkyl chains, respectively. These fSAMs are appended with fluorescein isothiocyanate (FITC), an anionic fluorescent motif, via a flexible tetraethylene glycol (TEG) linker. The carboxylate moiety of FITC head groups can bind, via the formation of multiple salt bridges, to the peripheral guanidinium ion (Gu⁺) pendants of a water-soluble dendritic guest (Gdn-Rho) with a rhodamine (Rho) dye at the core.⁶ I serendipitously found that fSAM_{C12} behaved quite differently from fSAM_{C2} in the voltage-responsive capture and release of Gdn-Rho. Further investigations using the series of fSAMs revealed that the salt bridge was progressively more resistant to protonolysis as it approaches the hydrophobic surface. This was interpreted to be clear evidence for the theory of Schellman.

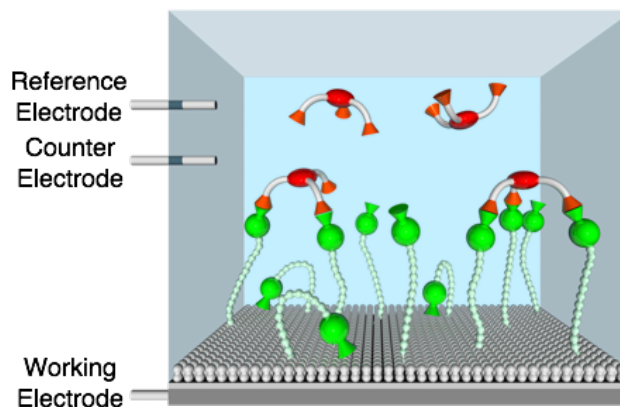


Figure 1. Illustration of voltage-responsive fSAM_{C2} capable of reversible capture and release of Gdn-Rho.

The first non-redox voltage-responsive self-assembled monolayer (SAM) was reported by Lahann *et al.* in 2003,⁷ where a charged distal motif, being attracted or repelled by an applied surface potential, induced a conformational change of surface-bound molecules. Nature indeed offers an alternative yet still simple idea other than electrostatics to realize non-redox voltage responsiveness: Reversible protonation of charged amino acids or embedded organic molecules is universally harnessed by membrane proteins for sensing voltage changes. Recent studies suggest that certain voltage-sensing G protein-coupled receptors (GPCRs) may employ reversible protonation of crucial acidic amino acids as an electrical switch to trigger conformational changes and control their binding affinities towards aminergic agonist ligands.⁸ Inspired by voltage-sensing GPCRs, I endeavored to create an artificial voltage-responsive monolayer capable of guest capture and release (Figure 1), where a charged motif was used to sense an applied voltage via its reversible protonation.

Chapter 1 Electric Field-Responsive SAMs: Visualization of Proton-Triggered SAM Behaviors in Response to an Applied Voltage

I started the monolayer design by conceiving a molecular motif that could respond to an electrically generated proton gradient. One of these molecules that came to my mind is FITC. Once located in a proton gradient, the hydrophobicity of FITC,⁹ along with its fluorescence emission,¹⁰ is tunable within a wide range. One facile way to generate a local proton gradient can be applying a voltage on an electrode in water.¹¹ Therefore, I attached FITC moieties at the termini of hydrophilic TEG chains that were anchored on the surface of a highly doped silicon wafer electrode via silanization to form a fluorescent SAM. Coassembly with space-filling hydrophobic ethyl chains gave fSAM_{C2}. The fabrication of fSAM_{C2} was confirmed by electronic adsorption, fluorescence, and X-ray photoelectron spectroscopies.

A challenge in my study lies with the quantitative, and real-time observation on the behaviors of SAMs under an applied voltage. For this purpose, I employed dedicated *in situ* analytical techniques. Front-face fluorescence spectroscopy was used to monitor the evolution of surface fluorescence emission in real time, while spectroscopic ellipsometry was employed to measure the variation of monolayer thickness. Homemade sample cells were designed, for both *in situ* analytical methods, to allow the assembly of a three-electrode electrochemical system.

fSAM_{C2} exhibited remarkable changes in fluorescence emission and ellipsometric thickness upon the application of alternating voltages of ± 1.5 V (vs. Ag/AgCl), which were properly in the non-redox potential window. When a voltage of +1.5 V (vs. Ag/AgCl) was

applied to fSAM_{C2} in water, the FITC emission at 513 nm upon excitation at 460 nm was significantly enhanced. In contrast, when the applied voltage was subsequently switched to -1.5 V (vs. Ag/AgCl), the fluorescence intensity fell off dramatically. Such a voltage-triggered evolution in fluorescence emission could be repeated as many as 10 cycles with little deterioration. This phenomenon is an apparent evidence for the reversible protonation and deprotonation of the FITC head groups.¹⁰ Of particular interest, fSAM_{C2} also underwent a thickness deviation synchronous to the polarity switching of the applied voltage. As evaluated by *in situ* ellipsometry, fSAM_{C2} changed its thickness from 1.2 nm to 0.3 nm when the applied voltage was switched from $+1.5$ V to -1.5 V (vs. Ag/AgCl), and vice versa. The timescale of this phenomenon was comparable to that of the voltage-responsive fluorescence variation. In order to understand the transition behavior of fSAM_{C2}, I prepared fSAM_{C12}, whose space-filling dodecyl chains are much longer than those of fSAM_{C2} but the FITC head groups are designed to remain unchanged. fSAM_{C12} likewise showed voltage-responsive behaviors. However, compared with the case of fSAM_{C2}, the range of fluorescence variation was obviously narrower and the time to reach a plateau is much shorter. Also noteworthy, the thickness of fSAM_{C12} was totally intact to a polarity change of the applied voltage.

The interesting differences in the voltage-responsive behaviors of fSAM_{C2} and fSAM_{C12} signify a specific potential for fSAM_{C2} to undergo conformational transitions driven by local hydrophobic interactions. The FITC-TEG molecules in fSAM_{C2} are supposed to possess a certain freedom in conformational change.⁷ Therefore, when the FITC head groups lose their ionic character by protonation at -1.5 V (vs. Ag/AgCl), an enhancement of hydrophobic interactions at the FITC head groups leads to the contraction of fSAM_{C2}.⁹ Consequently, the fluorescence of FITC is quenched by, in addition to its protonation,¹⁰ an enhanced distance-dependent nonradiative energy transfer to the electrode.¹² In contrast, the FITC head groups of fSAM_{C12} are surrounded by densely packed dodecyl chains. Hence, even after the FITC head groups are protonated, fSAM_{C12} hardly undergoes a conformational transition due to steric hindrance,⁷ which also prevents additional quenching of its fluorescence emission by the electrode.¹² In support of the above interpretation, I varied the pH of the environment of fSAMs externally and confirmed that fluorescence intensities of both SAMs decreased sigmoidally as the applied pH decreased. However, analogous to the voltage-responsive fluorescence change, fSAM_{C2} displayed a broader range of fluorescence intensity change than fSAM_{C12} as a result of its activity in contraction.

Molecular dynamics (MD) simulations were also performed to model the electric

field-induced conformational transition behaviors of fSAMs. The thickness deviation of fSAM_{C2} under opposite voltages is calculated to be 0.75nm. As for the fSAM_{C12} system, the calculated thickness change is only 0.03nm. The MD simulations are thus well consistent with the experimental observations.

Chapter 2 Sub-nanoscale Hydrophobic Modulation of Salt Bridges in Aqueous Media

Next, I wonder whether an electrical control of molecular interactions can bring about even more sophisticated functions such as molecular recognition activity. I envision that fSAM_{C2} and fSAM_{C12} may exhibit distinct recognition patterns towards a guest molecule due to a difference in their local hydrophobicity of the surroundings of the guest-binding site.

Regarding the guest-binding site, I designed a specific salt bridge interaction. A dendritic guest molecule, Gdn-Rho, bearing three Gu⁺ pendants⁶ was conceived to allow the formation of multivalent salt bridges with the carboxylate groups in the FITC moieties of fSAMs. In order to observe the voltage-regulated guest recognition behaviors of fSAMs, I attached a Rho dye to the focal core of the dendritic guest. Once the ligand was captured by fSAMs, fluorescence resonance energy transfer (FRET) took place from FITC to Rho so that an emission at 584 nm due to Rho was enhanced at the expense of that at 513 nm due to FITC. Binding of Gdn-Rho on fSAM_{C2} appeared to be strong since the FRET profile hardly changed upon rinsing with water.

Intriguingly, fSAM_{C2} and fSAM_{C12} exhibited distinct patterns in voltage-responsive ligand binding behaviors. For fSAM_{C2} incubated with Gdn-Rho, when a negative voltage of -1.5 V (vs. Ag/AgCl) was applied, an obvious decrease in Rho emission at 584 nm, along with an increase in FITC emission at 513 nm, was observed. This result indicates that the FRET from FITC to Rho was turned off as a consequence of the release of Gdn-Rho from fSAM_{C2}. Subsequently, I applied a positive voltage of $+1.5$ V (vs. Ag/AgCl), whereupon a spectral change, totally opposite to the above, was observed. Hence, fSAM_{C2} again captured Gdn-Rho. Such guest capture and release events could be repeated multiple times by switching the polarity of the applied voltage. In sharp contrast, fSAM_{C12}, under conditions identical to those for fSAM_{C2}, was totally inactive for voltage-responsive guest release. Even upon prolonged application of a negative voltage of -1.5 V (vs. Ag/AgCl), no change in the FRET profile resulted.

The contrasting voltage-responsive behaviors of fSAM_{C2} and fSAM_{C12} in guest recognition highlight a significant effect of local hydrophobicity on interfacial salt bridges. The salt bridges, formed between fSAM_{C12} and Gdn-Rho, are hydrophobically protected by the densely packed dodecyl chains, which are clearly evidenced by the requirement of a lower pH

for their protonolysis: The release of Gdn-Rho from fSAM_{C12} took place at pH 3.1, which was much lower than an applied pH of 4.9, at which fSAM_{C2} released Gdn-Rho. I estimated the binding free energy of the fSAM/Gdn-Rho conjugates based upon the Clausius–Clapeyron equation. Strikingly, the free energy of guest binding for fSAM_{C12} is as much as 3.9 kcal/mol greater than that for fSAM_{C2}. Thus, the stability of the salt bridge increases by as much as 3.9 kcal/mol when the distance of the binding site from the hydrophobic surface decreases by 1.0 nm. This value is approximately twice as large as the free energy of a typical hydrogen bond.

To systematically investigate how the strength of the salt bridge changes with increasing distance from the hydrophobic surface, I studied fSAM_{C6} and fSAM_{C8} having hexyl and octyl as space-filling alkyl chains, respectively. Binding free energies of fSAM_{C2}, fSAM_{C6}, fSAM_{C8}, and fSAM_{C12}/Gdn-Rho conjugations were calculated from their titration profiles, where the binding stability of the guest increases nonlinearly in an upwardly convex manner when its distance from the hydrophobic surface decreases from 1.2 to 0.8, 0.6, and 0.2 nm. This experimental result agrees well with two sets of MD simulations, one using real and the other using simplified models of the fSAM/Gdn-Rho conjugates. Both simulations show that the salt bridge-mediated guest binding is stabilized with the increase of the background alkyl chain length. Therefore, my study has provided solid experimental evidence for the Schellman's theory⁵ on the hydrophobic modulation of ionic interactions on a sub-nano scale.

Chapter 3 SAM Wetting Dynamics

In practice, freshly prepared SAMs are immediately forwarded to property characterizations or functional applications upon their exposure to solvents, based on a conventional understanding that wetting of SAMs costs only nanoseconds to seconds. The present knowledge on the time scale of SAM wetting basically originates from MD simulations or macroscopic observations of the profile changes of surface drop, both of which, in fact, fail to provide a molecular-level view of the SAM wetting process.

Here I employed the dedicated *in situ* fluorescence spectroscopy to study SAM wetting dynamics. Surprisingly, I discovered an unexpected long (>10 hours) water wetting process of fSAM_{C2}. The result suggests that, in the microscopic point of view, wetting dynamics of an ionic SAM in aqueous solution can be surprisingly slower than ever thought before. In order to support this finding, I also applied time-resolved *in situ* infrared reflection inspection and *in situ* ellipsometry during the SAM wetting process. Both methods confirmed the relaxation of the molecular chains and the diffusion of water molecules during wetting. Furthermore, I found that

solvent conditions, such as different polarities and ionic strengths, have a large effect on the wetting dynamics.

Concluding Remarks and Perspectives

I have presented a clear experimental evidence for a 60-year-old theoretical prediction⁵ that ionic interactions are significantly enhanced when getting close to a hydrophobic surface, through the use of elaborately designed SAMs that capture a dendritic guest via multiple salt bridges, and quantitatively demonstrated that such a hydrophobic modulation operates in a distance-dependent manner on the sub-nanoscale. This theory would hopefully contribute to the understanding and interpretation of various molecular recognition phenomena in biological systems. Also, my study represents an initial step of integrating local hydrophobic interactions, on a nanoscale interface, into synthetic chemistry for realizing diverse adaptive functions. This design principle should be applicable to the creation of more complex ‘living’ materials.

References

- [1] D. Chandler, *Nature* **437**, 640–647 (2005).
- [2] W. Kauzmann, *Adv. Prot. Chem.* **14**, 1–63 (1959).
- [3] M. F. Perutz *et al.*, *J. Mol. Biol.* **13**, 669–678 (1965).
- [4] P. W. Snyder *et al.*, *Eur. Phys. J. Special Top.* **223**, 853–891 (2014).
- [5] J. A. Schellman, *J. Phys. Chem.* **57**, 472–475 (1953).
- [6] Q. Wang *et al.*, *Nature* **463**, 339–343 (2010).
- [7] J. Lahann *et al.*, *Science* **299**, 371–374 (2003).
- [8] X. C. Zhang *et al.*, *Protein Cell* **4**, 747–760 (2013).
- [9] H. Diehl, R. Markuszewski, *Talanta* **32**, 159–165 (1985).
- [10] M. M. Martin, L. Lindqvist, *J. Lumin.* **10**, 381–390 (1975).
- [11] A. J. Bard, L. R. Faulkner, *Electrochemical Methods: Fundamentals and Applications* (John Wiley & Sons, 2001).
- [12] A. P. Alivisatos *et al.*, *J. Chem. Phys.* **86**, 6540–6549 (1987).

Publication

Chen S, Itoh Y, Masuda T, Shimizu S, Zhao J, Ma J, Nakamura S, Okuro K, Noguchi H, Uosaki K, Aida T. Sub-nanoscale hydrophobic modulation of salt bridges in aqueous media. *Science* Accepted (2015).